Geochemistry Geophysics Geosystems G3
AN ELECTRONIC JOURNAL OF THE EARTH SCIENCES
Published by AGU and the Geochemical Society

Article
Volume 6, Number 9
8 September 2005
Q09006, doi:10.1029/2005GC000917
ISSN: 1525-2027

On the relationships between slab dip, back-arc stress, upper plate absolute motion, and crustal nature in subduction zones

Serge Lallemand and Arnauld Heuret
Laboratoire de Dynamique de la Lithosphère, UMR 5573 CNRS-UM2, Université Montpellier 2, CC. 60, Place E. Bataillon, 34095 Montpellier Cedex 5, France (lallem@dstu.univ-montp2.fr; heuret@dstu.univ-montp2.fr)

David Boutelier
Department of Geology, University of Toronto, 22 Russel Street, Toronto, Ontario, Canada M5S 3B1 (boutelier@geology.utoronto.ca)

[1] Statistical analysis of modern oceanic subduction zone parameters, such as the age of a downgoing plate or the absolute plate motions, is performed in order to investigate which parameter controls the dip of a slab and, conversely, what the influence of slab geometry is on upper plate behavior. For that purpose, parameters have been determined from global databases along 159 transects from all subduction zones that are not perturbed by nearby collision or ridge/plateau/seamount subduction. On the basis of tomographic images, slabs that penetrate through, or lie on, the 670 km discontinuity are also identified. The results of the statistical analysis are as follows: (1) Back-arc stress correlates with slab dip, i.e., back-arc spreading is observed for deep dips (deeper than 125 km) larger than 50°, whereas back-arc shortening occurs only for deep dips less than 30°. (2) Slab dip correlates with absolute motion of the overriding plate. The correlation is even better when the slab lies on, or even more penetrates through, the 670 km discontinuity. (3) Slabs dip more steeply, by about 20° on average, beneath oceanic overriding plates than beneath continental ones. (4) Slabs dip more steeply on average by about 10° near edges. (5) Slab dip does not correlate with the magnitude of slab pull, the age of subducting lithosphere at the trench, the thermal regime of the subducting lithosphere, the convergence rate, or the subduction polarity (east versus west). The present study provides evidence that the upper plate absolute motion plays an important role on slab dip, as well as on upper plate strain. Retreating overriding plates are often oceanic ones and thus may partially explain the steeper slab dips beneath oceanic upper plates. One can infer that low slab dips correlate well with compression in continental advancing upper plates, whereas steep dips are often associated with extension in oceanic retreating upper plates. Excess weight of old slabs is often counterbalanced by other forces, probably asthenospheric in origin, such as lateral mantle flow near slab edges or anchor forces, to determine slab dip.

Components: 12,676 words, 13 figures, 1 table.

Keywords: slab dip; subduction dynamics.

Index Terms: 3040 Marine Geology and Geophysics: Plate tectonics (8150, 8155, 8157, 8158); 3060 Marine Geology and Geophysics: Subduction zone processes (1031, 3613, 8170, 8413); 8120 Tectonophysics: Dynamics of lithosphere and mantle: general (1213).

Received 13 January 2005; **Revised** 19 May 2005; **Accepted** 6 June 2005; **Published** 8 September 2005.

Lallemand, S., A. Heuret, and D. Boutelier (2005), On the relationships between slab dip, back-arc stress, upper plate absolute motion, and crustal nature in subduction zones, *Geochem. Geophys. Geosyst.*, *6*, Q09006, doi:10.1029/2005GC000917.

1. Introduction

[2] Upper plate strain is known to have some relation with slab dip. Low-angle subduction is thought to greatly facilitate the transmission of compressive stress to the overriding plate through increased contact area between the plates [e.g., *Barazangi and Isacks*, 1976; *Jordan et al.*, 1983]. *Ruff and Kanamori* [1980] noticed that strain regime is positively correlated with shallow dip and inversely correlated with deep dip. On the other hand, *Jarrard* [1986] concluded from a statistical analysis of data available at that time that strain class was probably determined by a linear combination of convergence rate, slab age and shallow slab dip. Regarding the control of slab dips, *Hager and O'Connell* [1978] suggested that mantle flow can explain most slab dip angles by lateral pressure on the slab.

[3] A preliminary study performed 5 years ago by one of the coauthors, David Boutelier, revealed that any active back-arc shortening was associated with slab dips at depths of more than 100 km, shallower than 50°, and conversely, any active back-arc spreading was associated with deep slab dips steeper than 50° (Figure 1). This work was done using a limited but representative set of transects. Such first-order observations apparently questioned some of the former conclusions. We thus suspect some relation between slab dip and upper plate strain regime, but (1) is the relation simply linear between the two characteristics, or does it involve other parameters? (2) If such a relation exists between slab geometry and upper plate strain, which one is the controlling parameter?

[4] On the other hand, many authors consider that the slab dip is mainly influenced by the slab pull, e.g., Chilean-type versus Mariana-type [*Uyeda and Kanamori*, 1979]. Such a correlation is indeed verified along some subduction zones like South Chile or Nankai (young subducting plates and low-angle subduction) or Mariana (old subducting lithosphere and steep-angle subduction). Furthermore, on the basis of the observation of a westward drift of the lithosphere with respect to the underlying asthenosphere, *Doglioni et al.* [1999] have suggested that W-dipping slabs should be steeper than E-dipping ones, because of the pressure exerted by mantle flow on the slabs. Unfortunately, both theories suffer from well-known counterexamples like the old Pacific plate subducting at a very-low angle beneath Northeast Japan or the young Atlantic lithosphere subducting at a very steep angle beneath Sandwich Islands. *Conrad et al.* [2004] concluded that subduction zone tectonics do affect plate-driving forces, such as slab pull. In this paper, we reassess the relation between slab dip, slab pull, plate velocities and the tectonic regime of the subduction, and challenge previous models.

[5] Our approach may be biased by the fact that we only examine present-day observations of subduction zones, which is obviously a limitation. Unfortunately, we cannot avoid this limitation as any reconstruction of slab dip through time is very speculative and cannot be used for robust conclusions. On the basis of numerical and analogical experiments, we are fully aware that slab dips evolve through time at rates comparable to, or even larger than, those of plates motions. Bearing this limitation in mind, we explore the spectrum of present-day subduction zones and try to better constrain the processes in action.

2. General Context

[6] Regarding the main forces that influence both the plates kinematics and deformation in a subduction zone (Figure 2), we identify the slab pull force, defined as the mass excess of the slab relative to the surrounding mantle, the viscous resistance of the mantle during the sinking of the slab as well as the forward or rearward motion of the slab (anchor force), the viscous shear force during slab penetration, the coupling between the plates along the interplate zone, which includes both the interplate friction and pressure and the bending/unbending of the slab. Other sources of stress (difficult to estimate) are also acting, such as the regional mantle flow or the corner flow. The combination of these forces generates stresses in both the subducting and the overriding plates. In this paper, we will focus on those expressed in the upper plate because we have direct access to the deformation rates, through GPS measurements. This does not mean that the deformation within the subducting plate can be neglected. For example, regarding the poor correlation between estimated slab pull and plate kinematics [*Conrad and Lithgow-Bertollini*, 2002], *Conrad et al.* [2004] concluded that a number of slabs may be considered as detached from the subducting plate, due to strong intraplate deformation.

3. Data Set

[7] *Jarrard*'s [1986] statistical analysis of subduction zones was based on 26 parameters

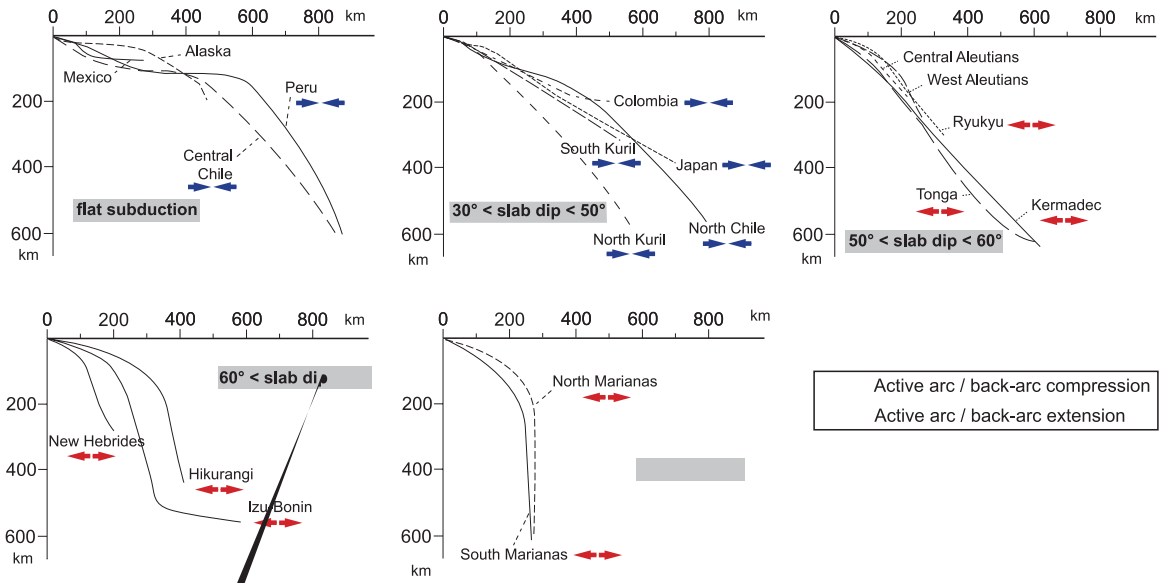

averaged over 9 segments of roughly constant subduction conditions. Since this earlier exhaustive study, there has been a general improvement of available data, both in accuracy and in the homogeneity of sources, with the advent of global data sets like the *Engdahl et al.* [1998] relocated hypocenter catalogue (EHB98) or the digital ocean floor age grid of *Müller et al.* [1997]. Moreover, new constraints on slabs geometries, especially in their deeper parts, are provided by the recent development of seismic tomography. All of these improvements allow a new examination of slab dips statistical features.

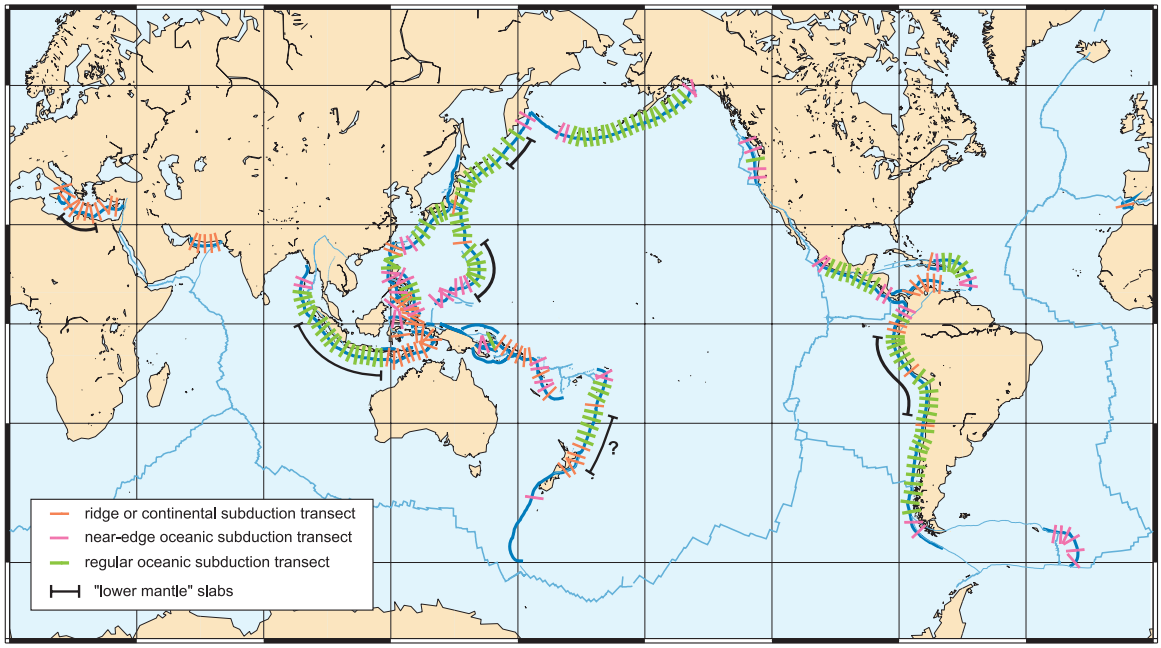

Figure 3. Location of the 245 transects over all subduction zones. Those in orange are not used in the present study because they are close to collision zones or ridge or plateau subduction. The remaining 159 transects are divided into 114 regular ones in green and 45 near-slab edge transects in pink. Thick black lines outline regions where slabs penetrate into the lower mantle based on tomography.

[8] The present statistical study is based on a selection of 159 "nonperturbed oceanic subduction" transects among the 245 we have compiled checking about 50 parameters. We define "nonperturbed oceanic subduction" as any subduction of an oceanic plate beneath another plate (continental or oceanic) far from any collision zone, ridge or plateau subduction (in green and pink in Figure 3). A collision zone means that a continental plate subducts beneath another plate. Such a geodynamic setting as well as ridge or plateau subduction is often accompanied by upper plate compression in the vicinity of the collision and extension or extrusion on the sides. The study of such regional effects needs special attention and are clearly beyond the scope of the present paper. We have used a sampling step of about 220 km of trench to extract the transects which represent nearly 36,000 kilometers of trenches. This uniform and systematic sampling has been chosen to better account for the lateral variations along apparent homogeneous subduction segments.

[9] We then identified three groups within this set (groups that could overlap; see Figure 3): (1) 114 "regular" in green; (2) 45 "near-edge" in pink when a transect is located within 400 km from the termination of a slab; and (3) 39 transects for which the slab penetrates into the lower mantle according to available tomographic images (hereafter called "lower mantle slabs"). These 39 transects include all continuous slabs with maximum depths exceeding 670 km, whether these are straight or curved near the mantle discontinuity.

[10] In this study, we will discuss ten basic parameters and six combinations of parameters which appear to be relevant to slab dip (Figure 4; Table 1).

[11] The geometry of the subducting plate is parameterized according to slab dip, maximum depth and length. Typically, slab dip increases gradually from the trench to a depth of 80–150 km. Beneath this depth, it remains almost constant down to the limit between upper and lower mantle where it may be deflected. After a careful examination of slab geometries, we have observed that the major change in dip occurs around 125 km depth. In order to minimize the subjective bias induced by the changes in slab dip, we have defined a mean shallow dip between 0 and 125 km called α_s and a mean deep dip for depths greater than 125 km called α_d. For most subduction zones, a "best fit" of the upper surface of the slabs can be made using the distribution of earthquakes' hypocenters. Trench-

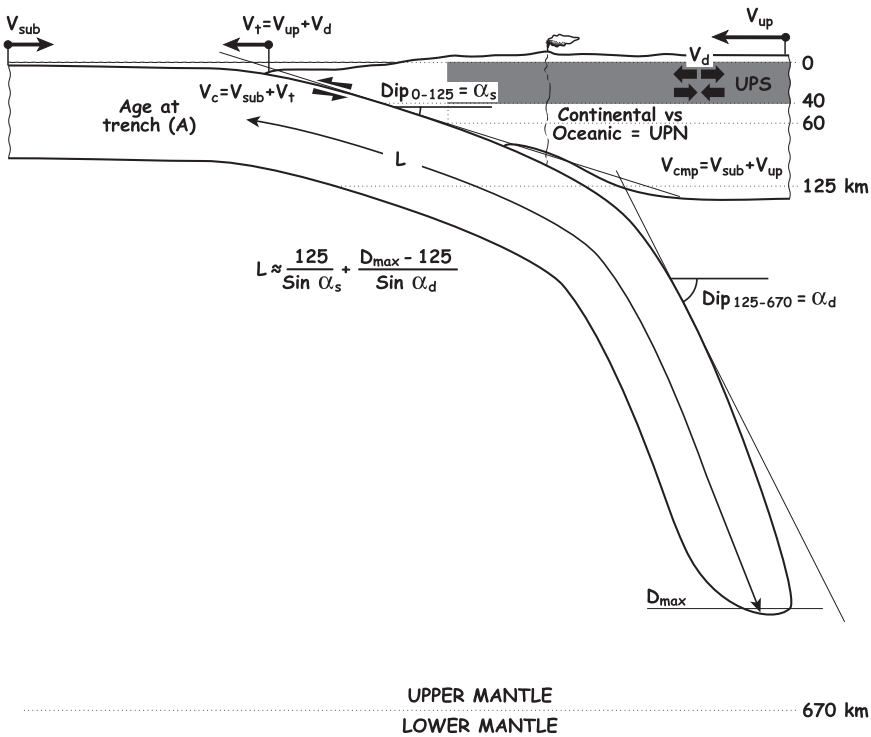

Figure 4. Schematic representation of the parameters used in this study. Absolute velocities of the subducting plate V_{sub}, of the trench/arc system V_t and of the upper plate V_{up}, are positive trenchward. The deformation rate in the back-arc region V_d is positive for spreading and negative for shortening. Maximum depth of the slab D_{max} is based on tomography and not seismicity. L is the slab length estimated from its maximum depth and mean dip. UPS, upper plate strain; UPN, upper plate nature. The gray pattern within the overriding plate is the sampling area for earthquakes which focal mechanisms are used for determining UPS class from E3 (active extension) to C3 (active compression).

normal cross sections of the seismicity were plotted for each 220 km of trench, using the EHB98 catalogue. Dips were measured using Benioff zones only for the ones (85%) that exhibit a sufficiently well defined upper boundary. Uncertainties have been estimated to about ±2.5° for 2/3 of the cross sections, and ±5° for the others. Concerning the remaining 15% of poorly defined slab geometries, we have used local seismicity studies in order to estimate α_s. This concerns low seismicity subduction zones like Manila [*Bautista et al.*, 2001], Nankai [*Xu and Kono*, 2002], Yap [*Fujiwara et al.*, 2000], Cascades [*Parsons et al.*, 1998], Mexico [*Pardo and Suàrez*, 1995], and Puysegur [*Eberhart-Phillips and Reyners*, 2001]. Tomographic data (see Table 1 for references) were used to estimate α_d when deep parts of slabs are aseismic. In this case, the uncertainty is about ±5°.

[12] Maximum slab depths D_{max} have also been measured on the basis of published tomographic profiles. It is clear that the degree of confidence varies from one study to another. For each subduction zone, we have thus chosen the most recent references and interpretations (listed in Table 1). A majority of profiles and interpretations come from *Fukao et al.* [2001], in which different wave models are objectively compared for each profile, and from *Bijwaard* [1999], which covers a wide range of subduction zones.

[13] Slab length L is calculated from α_s, α_d and D_{max} (see Figure 4). The length does not comprise the slab segments that lie on top of, or pass through, the 670 km discontinuity.

[14] We have estimated the age of slab A from the digital grid of *Müller et al.* [1997] averaging the subducting plate age on the first 10 km normal from trench (see *Heuret and Lallemand* [2005] for details). We consider that the error obtained for the slab age, using the approximation of age at trench is not worse than estimating the age of slab from reconstructions, because we were often confronted with various paleoreconstructions depending on authors.

[15] The upper plate strain (UPS) is determined from focal mechanisms of earthquakes occurring at

Table 1 (Representative Sample). Data Used in This Study[a] [The full Table 1 is available in the HTML version of this article at http://www.g-cubed.org]

Name	Lat., °N	Lon., °E	Az, °	α_s, °	α_d, °	D_{max}, km	Reference	L, km	V_{cn}	V_{cmpn}	V_{upn}	V_{tn}, mm.a^{-1}	V_{subn}	V_{zn}	A, Ma	φ, km	F_{sp}, 10^{12} N.m^{-1}	UPN	Slab Edge	UPS
ANDA6	14	92,1	112	50	*70*	600	*Replumaz et al.* [2004]	669	4	−20	−20	24	−22	3	86	269	20	c	y	E3
ANDA5	12	91,6	101	40	*70*	600	*Replumaz et al.* [2004]	700	7	−13	−1	24	−12	6	82	478	21	c	y	E3
ANDA4	10	91,4	97	37	*70*	600	*Replumaz et al.* [2004]	713	9	−10	−2	15	−7	8	78	602	21	c	n	E3
ANDA3	8	91,7	77	34	*70*	600	*Replumaz et al.* [2004]	729	18	3	−9	2	13	15	74	1092	21	c	n	E3
ANDA2	6	92,6	70	33	*70*	600	*Replumaz et al.* [2004]	735	18	5	−8	4	19	15	69	1006	20	c	n	0
ANDA1	4	93	61	33	56	600	*Replumaz et al.* [2004]	802	20	15	−13	−7	27	15	61	905	21	c	n	0
SUM6	2	95	25	29	*40*	1200	*Bijwaard* [1999]	1106	41	41	−18	−18	57	25	52	1290	26	c	n	0
SUM5	0	97	56	28	*40*	1200	*Bijwaard* [1999]	1114	28	28	−13	−13	38	17	46	786	25	c	n	0
SUM4	−2	98,1	47	28	49	1200	*Bijwaard* [1999]	988	37	37	−15	−15	46	25	47	1175	22	c	n	0
SUM3	−4	99,7	50	28	49	1200	*Bijwaard* [1999]	988	38	38	−13	−13	46	26	60	1541	25	c	n	0
SUM2	−5,5	100,8	51	28	61	1200	*Bijwaard* [1999]	889	39	39	−12	−12	47	29	69	2017	24	c	n	0
SUM1	−7	102,3	34	27	63	1200	*Bijwaard* [1999]	887	50	50	−15	−15	61	37	72	2692	25	c	n	0
JAVA7	−8,4	105	32	27	71	1200	*Bijwaard* [1999]	852	53	53	−15	−15	64	42	75	3133	24	c	n	0
JAVA6	−9,7	107	25	26	68	1200	*Bijwaard* [1999]	873	57	57	−15	−15	70	44	78	3430	25	c	n	0
JAVA5	−10,5	109	10	28	68	1200	*Bijwaard* [1999]	854	60	60	−16	−16	75	47	80	3766	25	c	n	0
JAVA4	−10,4	111	10	29	69	1200	*Bijwaard* [1999]	842	62	62	−15	−15	76	49	81	3998	25	c	n	0
JAVA3	−10,7	113	8	30	68	1200	*Bijwaard* [1999]	838	64	64	−15	−15	77	51	82	4197	25	c	n	0
JAVA2	−11,2	115	11	29	68	1200	*Bijwaard* [1999]	846	65	65	−14	−14	77	51	83	4274	25	c	n	0
JAVA1	−11,3	117	359	27	70	1200	*Bijwaard* [1999]	855	66	66	−13	−13	79	52	84	4336	26	c	n	0
SULA2	2	123	170	30	-	150	*Bijwaard* [1999]	270	36	56	80	49	−14	20	40	798	6	c	y	C1
SULA1	2,3	121	190	30	-	150	*Bijwaard* [1999]	-	26	23	80	37	−11	-	40	-	-	c	y	C1
NEG	10	121,7	92	32	*55*	300	*Lallemand et al.* [2001]	450	25	97	94	20	−4	17	20	332	7	c	y	C1
LUZ4	14	119,2	65	*40*	*75*	400	*Lallemand et al.* [2001]	479	41	65	54	34	11	34	22	753	7	o	y	C1
LUZ3	16	119,2	95	*36*	*60*	670	*Lallemand et al.* [2001]	842	71	93	54	68	7	56	18	1017	12	o	y	C1
LUZ2	17,5	119,2	88	*26*	*60*	670	*Lallemand et al.* [2001]	914	86	87	80	81	9	63	27	1705	16	o	n	C1
LUZ1	19	119,8	119	*37*	*65*	670	*Lallemand et al.* [2001]	809	97	96	96	94	2	80	32	2565	15	o	n	C1
BAT	20,5	120,2	74	*41*	*75*	670	*Lallemand et al.* [2001]	755	70	70	60	60	12	62	35	2172	15	o	n	C1
PHIL6	4	128,6	246	39	-	250	*Bijwaard* [1999]	-	16	77	7	−57	72	-	50	-	-	c	y	C1
PHIL5	8	127,3	267	35	-	250	*Bijwaard* [1999]	330	37	95	6	−62	92	28	50	1413	8	c	n	C1
PHIL4	10	126,8	253	36	-	250	*Bijwaard* [1999]	330	36	80	9	−44	74	28	50	1375	8	c	n	0
PHIL3	12	126,2	247	34	-	250	*Bijwaard* [1999]	300	42	71	10	−19	65	35	50	1767	7	c	n	0
PHIL2	14	125,2	248	33	-	150	*Bijwaard* [1999]	270	53	70	11	−4	63	29	45	1323	6	c	y	0
PHIL1	15,6	123,5	205	30	-	100	*Bijwaard* [1999]	250	36	2	14	52	−9	14	40	578	5	c	y	0
RYU1	23,4	124	345	37	65	670	*Fukao et al.* [2001]	809	96	51	−14	30	64	79	35	2774	16	c	y	E3
RYU2	24,2	127	325	34	57	600	*Fukao et al.* [2001]	790	85	56	−18	9	77	65	38	2453	16	c	y	E2
RYU3	25,7	129	320	34	58	350	*Fukao et al.* [2001]	489	87	55	−21	12	76	62	48	2973	11	c	n	E2
RYU4	27,5	130,5	310	35	61	325	*Fukao et al.* [2001]	447	82	53	−21	7	74	60	50	2984	10	c	n	E2
RYU5	29,8	132	300	39	64	300	*Fukao et al.* [2001]	393	73	48	−21	9	70	55	50	2772	9	c	n	E2

[a] See the main text for details. 159 "oceanic subduction" transects are listed. In the column related to "upper plate nature" (UPN), c means continental, and o means oceanic. In the column related to "slab edge," y means yes and n means no. In the column related to "upper plate strain" (UPS), 0 means neutral, C means compressive, and E means extensive. The scale from active back-arc spreading to active back-arc compression is thus E3-E2-E1-0-C1-C2-C3.

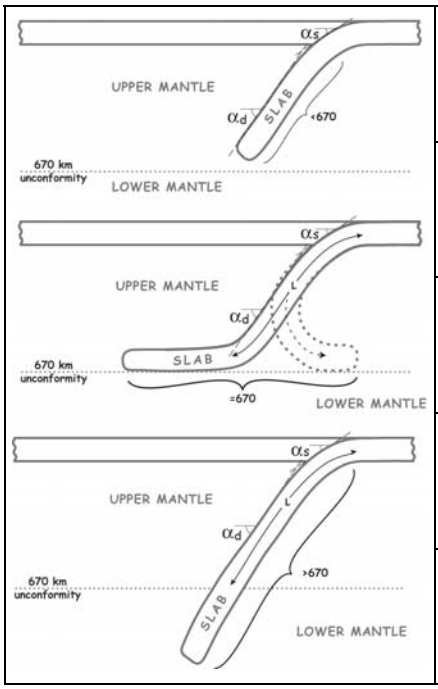

	α_s		α_d		
	R	Nb of transects	R	Nb of transects	
V_{up} vs α	-0.88	39	-0.75	39	**> 670**
	-0.70	65	-0.41	61	**≥ 670**
	-0.61	114	-0.39	89	**all slabs far from edges**
	-0.33	159	-0.26	117	**all slabs**
V_t vs α	-0.93	39	-0.69	39	**> 670**
	-0.52	65	-0.24	61	**≥ 670**
	-0.47	114	-0.24	89	**all slabs far from edges**
	-0.10	159	-0.03	117	**all slabs**
V_{sub} vs α	0.85	39	0.63	39	**> 670**
	0.57	65	0.10	61	**≥ 670**
	0.42	114	0.10	89	**all slabs far from edges**
	0.14	159	-0.06	117	**all slabs**
V_c vs α	-0.36	39	-0.26	39	**> 670**
	-0.03	65	-0.26	61	**≥ 670**
	-0.06	114	-0.22	89	**all slabs far from edges**
	-0.05	160	-0.10	117	**all slabs**
V_{cmp} vs α	-0.49	39	-0.58	39	**> 670**
	-0.44	65	-0.64	61	**≥ 670**
	-0.33	114	-0.55	89	**all slabs far from edges**
	-0.35	159	-0.49	117	**all slabs**

Figure 5. Cross correlation between absolute and relative velocities and slab dips with correlation coefficient R for each group of transects defined by the maximum depth reached by the thermal slab and/or the proximity of a slab edge. Correlation coefficients larger than 0.5 are shaded.

depths less than 40 km within the upper plate far from the subduction interface (gray area in Figure 4; see also *Heuret and Lallemand* [2005] for details). Like *Jarrard* [1986], we distinguish seven strain classes from highly extensional (E3, active back-arc spreading) to highly compressional (C3, active back-arc thrusting).

[16] We distinguish two groups of overriding plates depending on their crustal nature (upper plate nature (UPN)), either continental or oceanic and two groups of slabs, as said above, depending whether we are far from slab edges or not (see above). We also used tomographic images (see Figure 5) to determine that 25% of slabs penetrate into the lower mantle (>670), 27% lie on top of the 670 km discontinuity (=670) and 48% do not reach the discontinuity (<670).

[17] We also cross-correlate slab dip and plates motions. We distinguish 3 absolute velocities using HS3-NUVEL1A kinematic model of *Gripp and Gordon* [2002]: V_{sub} for the subducting plate, V_{up} for the main upper plate and V_t for the trench/arc, making the assumption that growth or consumption of the active margin front is negligible. By using this hot spot reference frame, we assume that there is no net drift of the hot spots during the last 5.7 Ma. We also consider that the motions of the lower mantle are far less than those of the upper mantle because of the higher viscosity. All absolute velocities are defined as positive trenchward. We call V_c the relative convergence between plates by summing V_{sub} and V_t. and those between the major plates V_{cmp} by summing V_{sub} and V_{up} (see Figure 4). We thus calculate the effective convergence V_c at trench as well as the convergence between major plates V_{cmp}. In this study, we only use the normal component of the velocities: V_{subn}, V_{upn}, V_{tn}, V_{cn} and V_{cmpn}.

4. Cross Correlations Between Parameters

[18] Our slab dip data set covers 159 "nonperturbed oceanic subduction transects" with a mean value of shallow dip α_s which equals 32° ± 11°, a minimum of 10° beneath Peru and a maximum of 75° at Yap (Figure 6). The mean value of deep dip α_d is 58° ± 14° with a minimum of 25° beneath Japan and a maximum of 90° beneath Mariana islands. Because of the limited length of some slabs, we sample only 117 transects to get values

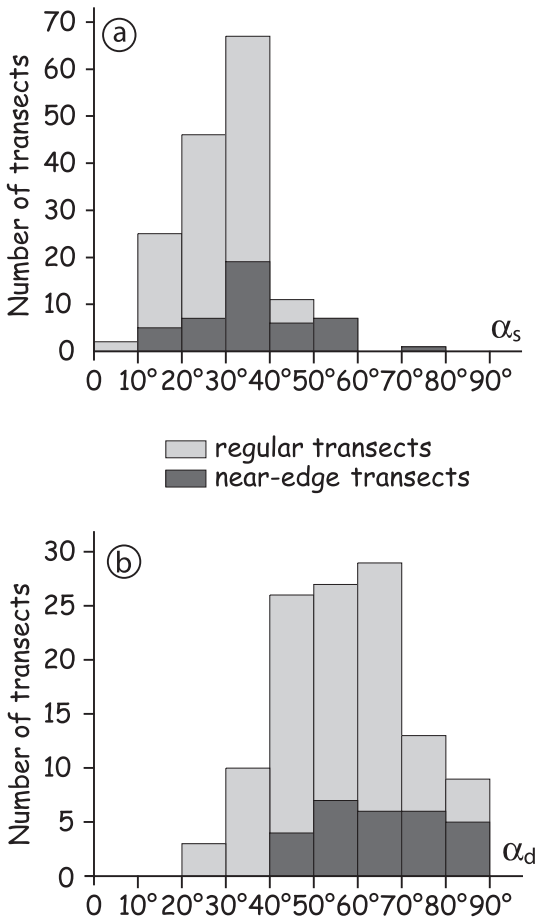

Figure 6. Distribution of (a) shallow and (b) deep slab dips α_s and α_d among the 159 "nonperturbed oceanic subduction transects." Near-edge transects systematically exhibit steeper dips.

of α_d. We observe a good correlation between α_s and α_d, with a coefficient R = 0,7.

[19] We observe steeper slabs near edges, i.e., α_s = 38° ± 13° (based on 45 transects) and α_d = 66° ± 12° (based on 28 transects). When removing "near-edge" transects, we observe lower values of α_s = 29° ± 9° (based on 114 transects) and α_d = 56° ± 14° (based on 89 transects). It thus appears that slabs are about 10° steeper in average near edges.

4.1. Slab Dip and Plate Kinematics V

[20] Following the earlier conclusions reached by *Luyendyk* [1970] (slab dip α is inversely related to V_c) or *Furlong et al.* [1982] (α is inversely related to V_{up}), we have examined the quality of the correlation between the slab dip and plates motions both relative and absolute. At first glance, we can conclude that the correlation coefficient is poor between any absolute or relative plate velocity and the slab dip ($|R| < 0.5$; see Figure 5). However, because we know that slabs geometries can be affected by edge effects, as well as slab penetration into the less mobile lower mantle, we have tested the same cross correlation within a set of 114 "oceanic transects far from slabs edges," which include 39 transects for which the slabs pass through the 670 km unconformity and 26 for which the slabs lie on top of the discontinuity.

[21] The result offers the best correlations for the absolute upper plate velocity V_{up} (Figure 7). We always observe a tendency for the slab dip to decrease with increasing upper plate velocity from negative to positive values. The correlation is better with α_s than α_d, and much better when the slab penetrates into the lower mantle: correlation coefficient |R| for linear regression equals 0.75 for α_d and 0.88 for α_s; it falls to 0.41 and 0.70, respectively, if we include slabs lying on the discontinuity and 0.39 and 0.61 for all slabs (see Figure 5).

[22] The best correlations are observed between slab dip and arc/trench absolute motion V_t, especially for "lower mantle" slabs ($|R| = 0.69$ for α_d and 0.93 for α_s), but the correlation rapidly deteriorates for other transects.

[23] A good correlation is still obtained for "lower mantle" slabs when comparing slab dip and subducting plate absolute motion V_{sub}, and, like V_t, it becomes worse for other transects. Slabs tend to dip more steeply for rapidly subducting plates.

[24] The correlation is poor between slab dip and V_c. The correlation improves when examining the convergence between major plates V_{cmp} rather than the effective convergence between the subducting plate and the arc V_c.

4.2. Slab Dip and Upper Plate Strain (UPS)

[25] As presented in the introduction, several authors infer that slab dip controls strain regime in the overriding plate (UPS). *Jarrard* [1986] treated that relation with caution and finally proposed that dip alone was an inadequate predictor of strain regime. We have used the same approach as Jarrard classifying all our 159 transects by strain characteristics within the upper plate from significant active extension (class E3) to significant active compression (class C3). Except for a few exceptions (Manila, Puysegur and Yap), the trend is clear both for α_s and α_d (Figure 8). For extreme classes, compression within the upper plate is

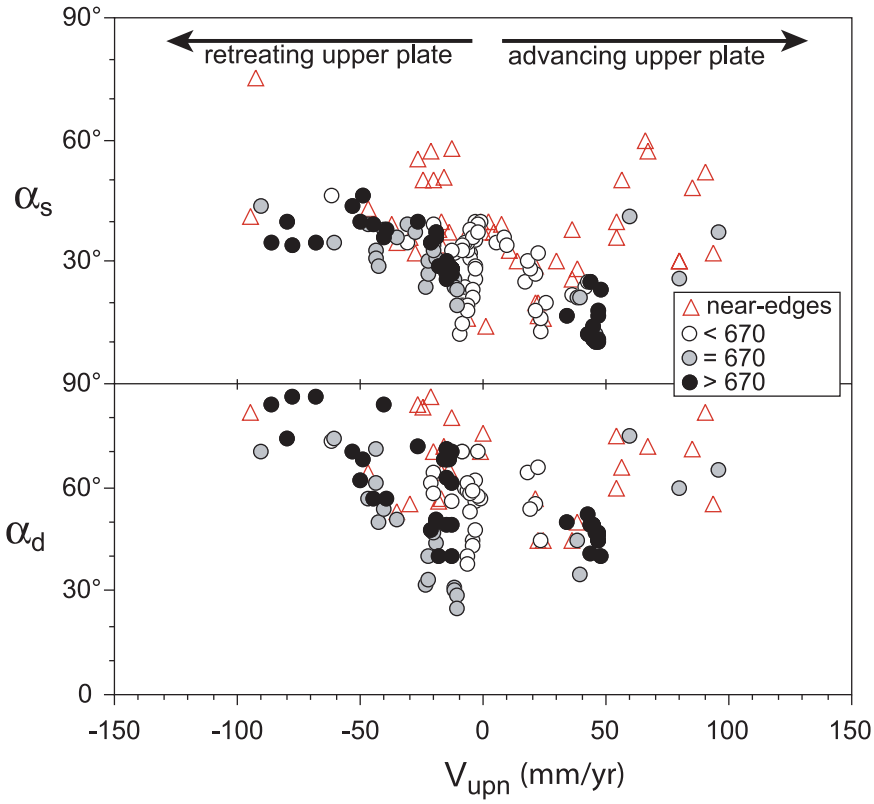

Figure 7. α_s and α_d as a function of the normal component of the absolute upper plate velocity V_{upn}. If we exclude near-edge transects (triangles generally showing steeper dips), we observe an inverse correlation between parameters, i.e., steeper dips for retreating upper plates. The best clustering is obtained for "lower mantle" slabs that penetrate into the lower mantle (>670 in black). See the text and Figure 5 for more details.

associated with low slab dips, whereas extension is always observed for steep slab dips. The threshold value is 31° ± 3° and 51.5° ± 0.5° for α_s and α_d, respectively. This is certainly the best correlation we have obtained that applies to almost all nonperturbed oceanic subduction transects. In order to illustrate the lateral variations of α_s along all subduction zones, we have used a color chart in Figure 9 to plot the shallow dips along trenches and located areas of active back-arc extension and compression.

4.3. Slab Dip and Slab Pull Force F_{sp}, Slab Age A, and Thermal Parameter φ

[26] It is widely accepted that the slab pull force acts on slab dip [*Vlaar and Wortel*, 1976; *Molnar and Atwater*, 1978]. We have tested this assumption using several methods. First, we have simply tested the relation between α_d and the age at trench A for all 117 nonperturbed oceanic subduction transects (Figure 10). One may think that deep slab dip α_d is appropriate to reflect slab pull effect, but we observe simply no relation at all between these two parameters even if we remove slab edges (28 transects) and/or "lower mantle" slabs (26 transects).

[27] Secondly, we have plotted the slab dip versus the slab pull force F_{sp} (Figure 11). We have used the definition of *Carlson et al.* [1983]: $F_{sp} = K.\Delta\rho.L.\sqrt{A}$. We set the constant K to 4.2 times g (gravitational acceleration = 9.81 $m.s^{-2}$) according to *McNutt* [1984], $\Delta\rho$ = 80 $kg.m^{-3}$ is the mean density difference between the slab and the surrounding asthenosphere, L is the slab length calculated only for the part above 670 km, and A being the slab age in Ma at trench. Again, we observe no relation at all between these two parameters, even when removing near-edge transects that generally exhibit larger dips. Looking carefully at various maximum slab depths, we observe a poor positive correlation with "upper mantle" slabs (<670), a good negative correlation with slabs that lies on top of the discontinuity (=670), and no correlation at all for "lower mantle" slabs that exhibit a wide range of dips for the same value of F_{sp} around 2.7 ± 0.5 10^{13} $N.m^{-1}$.

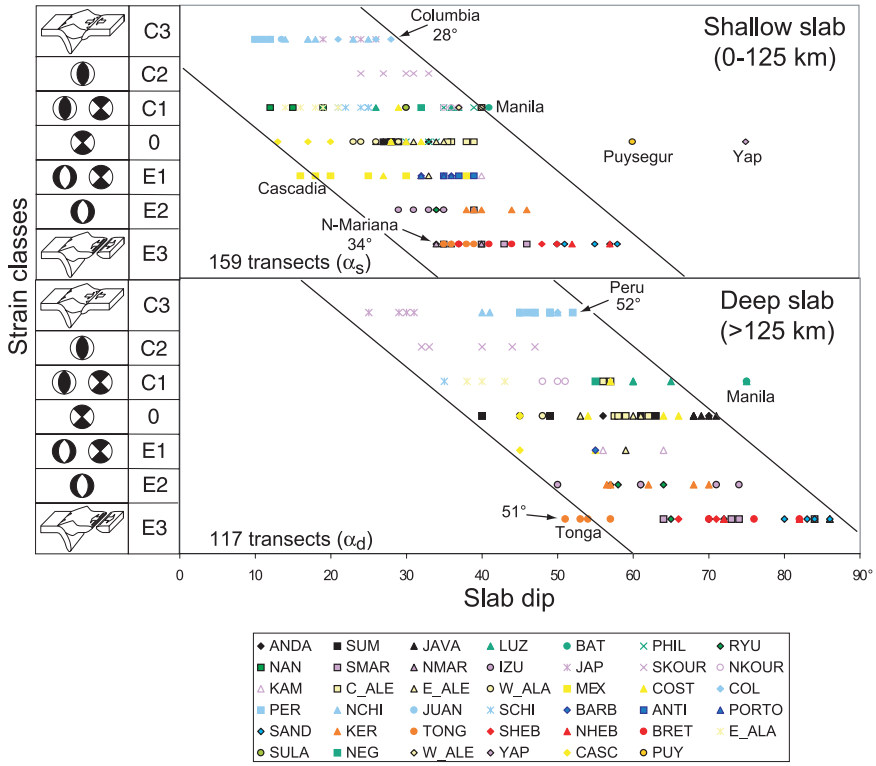

Figure 8. Correlation between slab dip and upper plate strain (UPS). See the main text for the determination of strain classes.

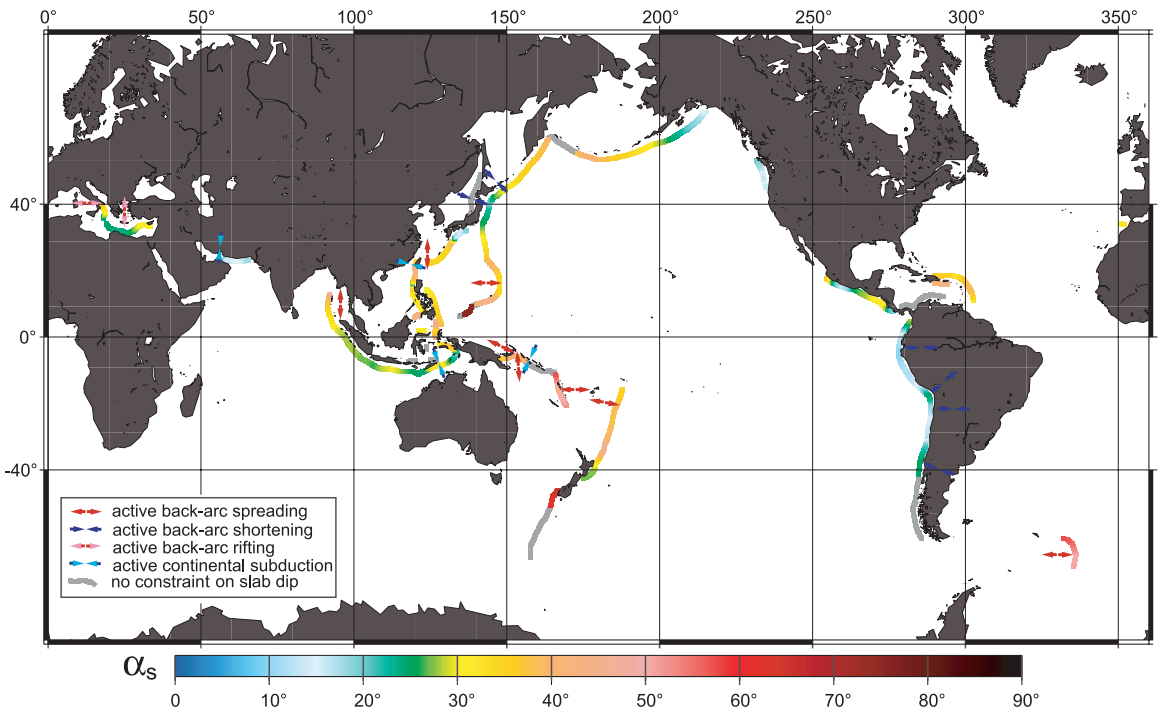

Figure 9. Distribution of shallow slab dips α_s with color scale.

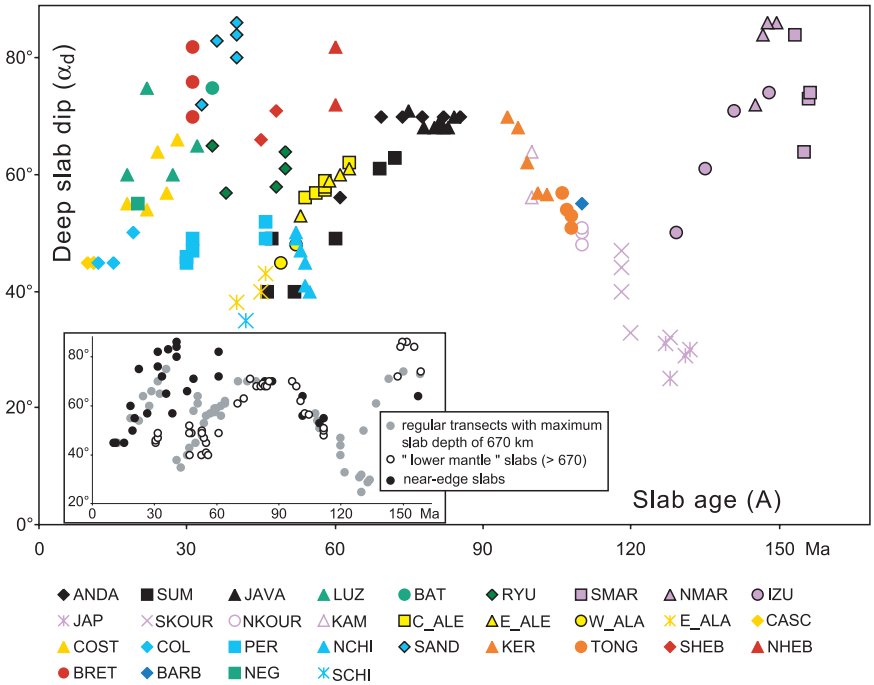

Figure 10. Deep slab dips α_d as a function of slab age at trench A along the 117 "nonperturbed" oceanic transects for which dip estimate was possible. The same data appear in the bottom left inset with special pattern for the 26 "lower mantle" slabs and the 28 "near-edge" slabs.

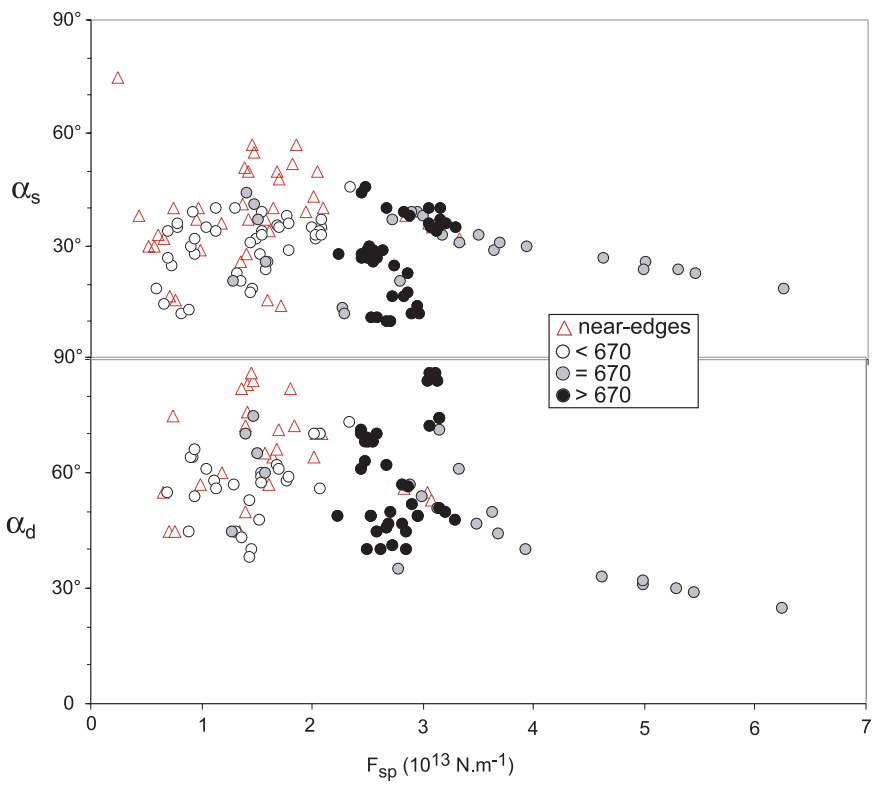

Figure 11. Plot of slab dip as a function of slab pull F_{sp}. If we exclude near-edge transects (triangles generally showing steeper dips), we observe no relation at all between these parameters. See text for details.

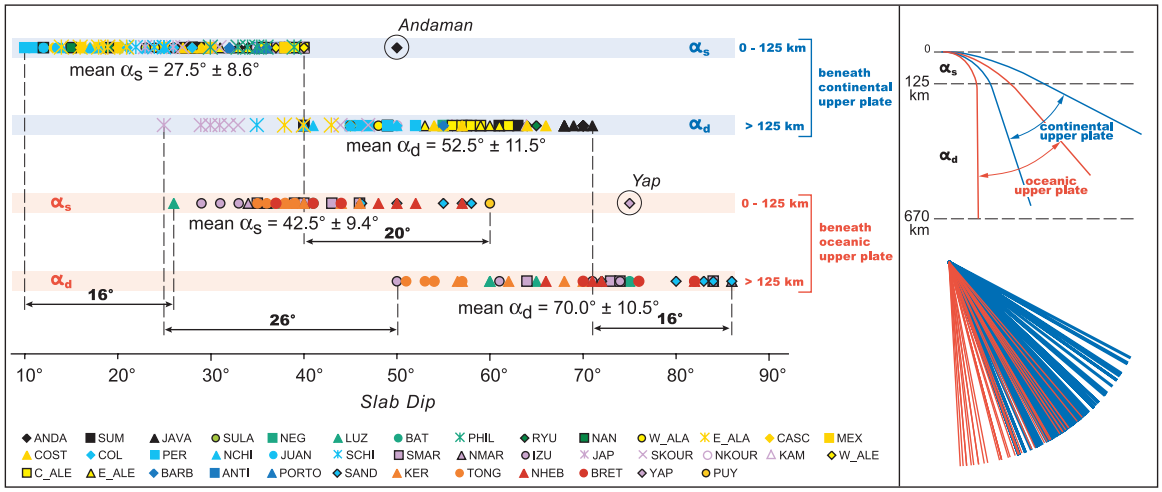

Figure 12. Plot of slab dips, alternately α_s and α_d, for (top) continental upper plates and (bottom) oceanic ones for the 159 "nonperturbed oceanic subduction transects."

The apparent negative trend in the right part of the diagram (Figure 11) for slabs lying on the discontinuity ($|R| = 0.33$ for α_s and 0.77 for α_d) exclusively concerns Japan and Kuril slabs. It shows that the dip shallows for higher values of slab pull (in fact when the length increases).

[28] Considering that mean slab density and rheology is controlled by its thermal state, we have finally tested the relation between α_d and the thermal parameter φ as defined by *Kirby et al.* [1996], as the product of A in Ma and the descent rate V_z in km.Ma^{-1}. Low φ characterizes warm slabs, whereas high φ corresponds to cold slabs. Again, it can be seen clearly that there is no relation between these parameters.

4.4. Slab Dip and Upper Plate Nature (UPN)

[29] *Furlong et al.* [1982], on the basis of 12 samples of subduction zones, noticed that the mean α_d is larger beneath oceanic (65°) than beneath continental (53°) overriding plates. Later, *Jarrard* [1986] improved the test using 29 transects and confirmed this tendency. He obtained 66° and 40.5°, respectively, as median α_d. In the present study, we have performed the same test with all 159 "nonperturbed oceanic subduction transects" (Figure 12). We definitely confirm that slabs dip more steeply beneath oceanic upper plates. The median α_d we obtained are 70 ± 10.5° (38 transects) for oceanic and 52.5 ± 11.5° (79 transects) for continental upper plates. α_s reach 42.5 ± 9.5° (42 transects) and 27.5 ± 8.5° (117 transects), respectively. Slabs dips are slightly lower when removing near-edge transects from the samples.

4.5. Slab Dip and Polarity of Subduction

[30] *Doglioni et al.* [1999], on the basis of the westward drift of the lithosphere relative to the mantle at the scale of the Earth, consider that the polarity of subduction is a major control parameter for subduction zones. In particular, one of the consequences is that W-directed slabs are thought to be steeper than E-directed ones.

[31] Our study shows that among the 159 "nonperturbed oceanic subduction transects," 47% of slabs dip eastward and 53% westward. Mean α_s is 28 ± 11° for eastward dipping slabs (74 transects) and 34 ± 10° for westward ones (85 transects). The difference is even less for α_d with 57 ± 12° versus 59 ± 16°, respectively. Looking at this small difference in slab dips, we have then excluded from our statistics all trench segments with azimuths between N45° and N135° as well as those between N225° and N315°. By doing this, we focus on slabs that should be affected at first by the eastward mantle wind. Finally, the dips are not much affected by this selection, i.e., 8 ± 11° of difference for α_s instead of 6 ± 11° and 5 ± 17° of difference instead of 2 ± 17° for α_d.

5. Discussion

5.1. Relation Between α and V_{up} and V_t

[32] Slab dip appears roughly correlated to both upper plate absolute motion V_{up} and trench abso-

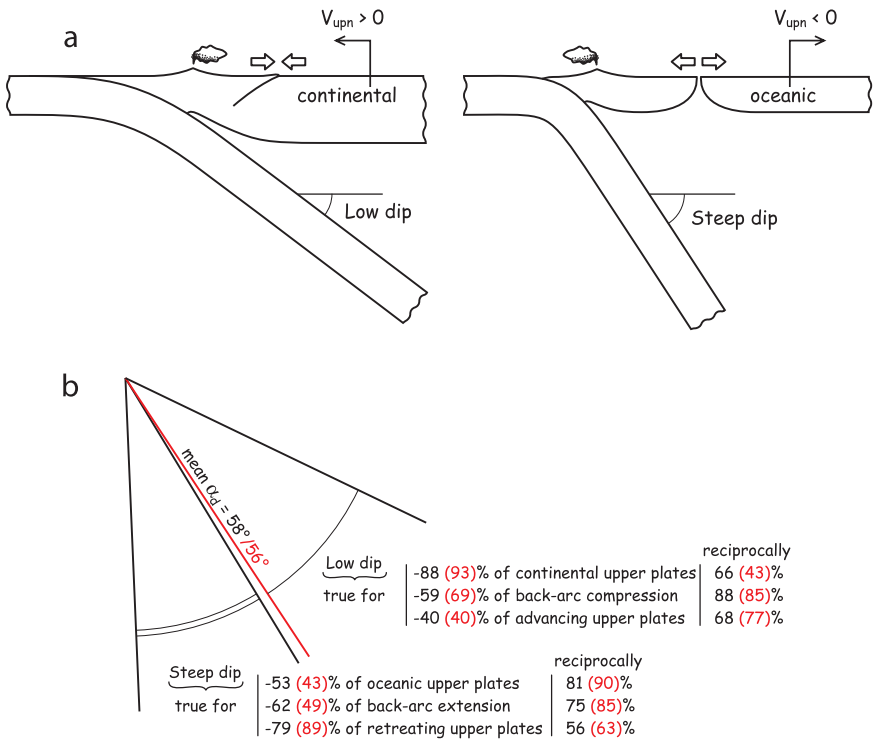

Figure 13. (a) Schematic end-members of subduction zones with parameter associations satisfied by more than 60% of "nonperturbed oceanic" subduction zones. (b) Real percentages of satisfaction between three parameters: UPN, UPS, and V_{upn} and slab dips less or larger than a mean value. The choice of this mean value is discussed in the main text: for all slabs in black and for transects far from slab edges in red.

lute motion V_t, especially for transects far from slabs edges. Advancing upper plates are associated with low slab dips, whereas retreating ones correlate with larger dips, and conversely for trench motions (Figure 13).

[33] By definition, the absolute trench motion V_t should be well-correlated with V_{up}, except when the upper plate significantly deforms (high V_d) because $V_t = V_{up} + V_d$. As the highest V_d occur near slab edges (e.g., Tonga, Sandwich, New Hebrides), trench motions more or less follow upper plates motions ($V_t \approx V_{up}$) for most transects located far from those edges [*Heuret and Lallemand*, 2005]. It is thus not surprising that V_t and V_{up} both correlate with slab dip when removing transects near slab edges.

[34] The mechanism which may explain such a correlation implies an almost "stationary" slab root at the deepest level, acting as a pivot with respect to subduction hinges which display motions controlled by V_{up}. The anchor force (viscous resistance to trench-normal slab migrations) may be responsible for this deep slab anchoring. Nevertheless, one must be cautious with this concept because *Heuret and Lallemand* [2005] had shown that the anchor force is inefficient to prevent trench migrations up to ±50 mm.y^{-1}. Figure 5 indicates that the statistical relation improves as the slab lies on, or even more penetrates through, the 670 km discontinuity. All these slabs are deflected, in a forward or in a backward direction [*Fukao et al.*, 2001] and may rest on the highly viscous lower mantle to accommodate trench migration thanks to changes in dip. Even if the exact mechanism is not clear according to these simple statistical observations and need to be tested by numerical and analogue modeling, we conclude that the upper plate motion might contribute to steepen the slab when the plate is retreating or flatten it when the plate is advancing.

[35] The apparent correlation between slab dip and V_{sub}, especially for "lower mantle slabs," is also observed by *Schellart* [2005] from a set of fluid dynamical experiments. He observes that hinge-retreat decreases with increasing subducting plate velocity under the conditions of the experiments (i.e., without overriding plate).

5.2. Relation Between α and UPS

[36] We have obtained one of our best correlations between UPS and both α_s and α_d (Figure 8).

Unlike Jarrard's conclusions, such a relation suffers from only a few exceptions for short slabs like Yap or Puysegur but no exceptions at all for extreme upper plate deformations, i.e., active back-arc spreading or active back-arc shortening.

[37] Let us first examine the case where the slab dip controls the UPS. Such a relation can be readily understood since we know that α_s has an effect on the degree of interplate coupling [*Cross and Pilger*, 1982; *Jarrard*, 1984; *Gutscher and Peacock*, 2003] through the area of friction between converging plates that increases when α_s decreases. Because α_d is generally well correlated with α_s, it is not surprising that the relation is satisfied for both slab dips. Another consideration pointed out by *Ranero et al.* [2003] is that oceanic faulting, when the slab bends prior to enter the subduction zone, may weaken it through mantle serpentinization and thus decrease its elastic behavior. In other words, steep shallow dips, by increasing the bending at outer rise, generates dense oceanic faulting that will reduce the unbending of the plate at depth and therefore contribute to steepen the slab.

[38] Strictly speaking, we should also examine the possibility of an opposite control, i.e., does UPS control the slab dip? It is quite difficult to evoke a causal and direct effect from UPS on the slab dip, but one can consider that upper plate compression is generally associated with strong plate coupling that generates a shear in a sense opposite to slab bending. Such opposite torque acting within the subducting plate below the frictional interface might diminish the slab bending. Another possibility comes from a recent numerical approach by *Conrad et al.* [2004], who suggested that strong plate coupling at subduction zones, that cause great earthquakes, weakens the slab and thus diminishes the slab pull effect. Such a weakened slab is then more susceptible to be deformed by the mantle wind, but in this case it can either increase or decrease the dip as a function of the direction of the mantle flow.

[39] Finally, we should remember that the correlation is rather good between α and V_{up} (see Figure 7 and section 5.1) and that V_{up} is generally well-correlated with UPS, i.e., compression for advancing upper plates and extension for retreating ones, except a few cases like Japan, Kuriles and New-Hebrides [*Heuret and Lallemand*, 2005]. Back-arc spreading is often associated with retreating upper plates ($V_{up} < 0$) and steep slab dips (high values of α). Thus we cannot exclude that V_{up} acts on both UPS and α.

5.3. Relation Between α and F_{sp}

[40] It has been shown that the absolute motion of the major plates is positively correlated with the donwndip length of subduction zones [*Forsyth and Uyeda*, 1975]. It is also accepted that the absolute motion of the subducting oceanic plates V_{sub} is positively correlated with the age of the lithosphere A [*Carlson*, 1995]. Gravity anomalies associated with subduction zones also indicate that slab pull must be a first-order force that drives the plates [e.g., *Ricard et al.*, 1991]. The relative speeds of subducting and nonsubducting plates is another piece of evidence supporting the slab pull force [*Conrad and Lithgow-Bertelloni*, 2002]. However, we have seen that neither A nor F_{sp} correlates with the slab dip, even when we test only slabs far from slab edges that do not reach the 670 km discontinuity. Does this mean that the excess mass of the slab, is not significant in the balance of forces that produce the observed geometry?

[41] In fact, slab pull predominance on subduction zone geometry is not so obvious. By definition, F_{sp} increases with L, but, at the same time, the viscous resistance of the upper mantle to slab penetration increases as well. This resistance to the slab sinking under its excess mass could prevent steep dip for long slabs. Bending force may also explain the lack of relation between slab dip and both A and F_{sp}. In fact, this resistive force is a function of the flexural rigidity of the subducting oceanic plate and increases as $A^{3/2}$, because it is proportional to the cube of the elastic thickness and the elastic thickness is often considered as proportional to the square root of the plate age [*Turcotte and Schubert*, 1982]. *Conrad and Hager* [1999] noticed that the viscous resistance to slab bending is also proportional to the cube of the slab thickness. As the excess mass increases with A, the bending force also increases making flexure of the plate more difficult. *Bellahsen et al.* [2005] have shown from experimental modeling that bending force could dominate on slab pull in the control of slab geometry (steepest slabs for thickest slabs). In natural subduction zones, the competition between bending and slab pull may partly explain the weak correlation observed between slab dip and subducting plate age. Another reason that tends to disrupt the correlation is suggested by *Conrad et al.* [2004] when they suggest that slab pull force for some slabs, associated with strong seismic coupling, might not be well transmitted to the surface plate anyway.

[42] In any case, we reach the conclusion that the slab pull force is counterbalanced by other forces originating from plate-motion-derived forces (influence of V_{sub} or V_{up} through viscous drag or resistance), mantle-flow forces (push), and/or age-dependent bending forces, to control the slab dip. It is also possible that the stress originated from slab pull is not fully transmitted to the surface plate.

5.4. Relation Between Slab Dip and UPN

[43] We confirm the result of previous studies revealing that slabs dip more steeply beneath oceanic plates and can quantify the mean difference to be about 20°. *Jarrard* [1986] proposed that the difference could be explained by a difference in duration of subduction between continental and oceanic overriding plates. To support his theory, he argued that slab dip correlated with the duration of subduction and that duration was greater for nearly all continental overriding plates than for oceanic ones. In this study, we did not compile the duration of subduction because we considered that there are great uncertainties regarding this parameter in many areas. Subduction erosion processes, for example, may consume remnants of volcanic arcs, or even that some earlier arc volcanics may be buried beneath younger rocks or water [e.g., *Lallemand*, 1998]. The question of the relation between duration of subduction and slab dip is less clear. *Jarrard* [1986] suggested some gradual heating of the overriding plate causing shallowing of dip with time, but such process has not been confirmed, at our knowledge, by any modeling. Among possible explanations for such an observation, we can evoke some variation in mantle viscosity [*Furlong et al.*, 1982; *Cadek and Fleitout*, 2003] or the fact that continental plates are thicker than oceanic ones. One may imagine that increasing the contact area between plates, promotes shallow dipping slabs by acting against the effects of slab bending through an opposite shear along the plates interface as suggested in section 5.2.

[44] We must also keep in mind that V_{up}, which is often positive for continental upper plates, is correlated with α. Mean V_{upn} for subduction beneath oceanic plates is -19 ± 56 mm/yr, whereas it is 6 ± 26 mm/yr for continental upper plates. Despite the scattering of the data, we observe that most oceanic upper plates retreat except in the New Hebrides or north of Luzon, but these two regions are probably affected by regional forces (collision, plume) that make them exceptions.

[45] Such complicated settings need to be tested through modeling before reaching any definitive conclusion.

5.5. Relation Between Slab Dip and Subduction Polarity

[46] We have seen that the concept for which W-directed slabs (like Mariana) dip steeper than E-directed ones (like Andes) is not supported by our data. This lack of correlation can be illustrated for example by the shallow dipping W-directed Pacific slab under Japan and the steeply dipping E-directed Cocos slab under Middle America. The difference in deep dip, i.e., $2 \pm 14°$, is not significant and those for shallow dip are only $6 \pm 10°$, which is also not significant. It appears that the difference in the nature of the upper plate, i.e., $15 \pm 9°$ for α_s and $18 \pm 11°$ for α_d, is more significant. We observe that more than 80% of E-directed slabs underthrust continental upper plates and, as mentioned above, most of them advance toward the trench. We thus think that the small difference in dip between E- and W-directed slabs is more likely due to either the nature or the absolute motion of the upper plate rather than the polarity of subduction.

5.6. Relation Between Slab Dip and Edge Proximity

[47] We have observed that slabs are 10° steeper on average near their edges. It is quite difficult to analyze this tendency since slab edges are not systematically steeper. Many slabs abut against collision zones or pass laterally either to highly oblique convergence or transform faults, prevent us from any global or definite conclusion. Those which significantly steeper dip edges are Andaman (north), Ryukyu (south), Izu-Bonin (south), Kamtchatka (north), Colombia (north) and Hikurangi (south). We also note that some of them dip more shallowly like Nankai (north), Mariana (north and south), Alaska (east).

[48] Slab edges are warmer than slab cores, generating adakitic arc magmas by melting of the subducting oceanic crust in some cases [*Yogodzinski et al.*, 2001]. Such local heating is susceptible to weaken the lithosphere and thus facilitate its bending. We can also attribute this observation to the effect of mantle flow-passing from one side of the slab to the other as indicated by mantle flow anisotropy in the northern Tonga or Kamtchatka for example [e.g., *Smith et al.*, 2001; *Yogodzinski et al.*, 2001], but in this case it can either produce a

shallowing or a deepening depending on the direction of flow motion.

5.7. General Tendencies

[49] We have tried to summarize in Figure 13 the general characteristics of the studied transects that exhibit either low or steep dips. To simplify, we only discuss slab dips deeper than 125 km: α_d. By doing so, we face a problem because we must choose arbitrarily a common "cutoff angle" between low and steep dips and we have seen above that this "divide angle" varies depending on the parameters studied. This angle is 50° for UPS, 55° for V_{upn}, and 62° for UPN. We have thus chosen the mean α_d = 58° for all slabs, or =56° if we remove "near-edge" transects. This choice slightly deteriorates the correlations but has the merit of using the same "cutoff angle" for several parameters.

[50] We can thus confirm that low slab dips better correlate with compressional continental advancing upper plates, whereas steep dips are often associated with extensional oceanic retreating upper plates (Figure 13a). When examining this correlation more closely, we notice that some correlations are better verified in one sense than in the opposite sense. If we try to quantify these general correlations (Figure 13b), we can say, for example, that 88% of the low dips characterize continental upper plates (93% if far from slab edges) and conversely, 66% of continental upper plates are characterized by low dips (58% if far from slab edges). Choosing the best sense for correlations, we can say that 81% of the steep dips characterize oceanic upper plates (90% if far from slab edges). Back-arc compression is observed for 88% of low dips transects, whereas back-arc extension is observed for 75% of steep dip transects. This last percentage would have increased up to 96% if we have used the limit of 50.5° rather than 58° described in section 4.2. Another reason why the correlation is not as good as described in section 4.2 is that neutral regime transects are taken into account in these percentages. 68% of advancing upper plates are associated with low slab dips (77% if far from slab edges), and 79% of the steep dips correspond to retreating upper plates (89% if far from slab edges).

[51] It often appears in our tests that some subduction zones systematically violate these general tendencies. These are New Hebrides, North Luzon, Yap, Puysegur, Andaman. All these subduction zones occur within specific geodynamic contexts that can, at least partially, explain their particular behavior. New Hebrides belong to a young arc that has rapidly rotated clockwise during the last 12 Ma as the result of the opening of the North Fiji basin above a regional mantle plume [*Lagabrielle et al.*, 1997]. The North Luzon arc is dual above a contorted slab that probably results from a complex recent history [e.g., *Yang et al.*, 1996]. Yap, Puysegur and Andaman are, all three, characterized by short slabs that deepen in a context of extremely oblique subduction. Given the specific context of these subduction zones, we had the choice of omitting them from our study or simply to include them. We chose to keep them because we did not want to add regional specificities to global ones such as the proximity of collision, slab edge or the maximum depth of slab penetration. It is clear that our results would make a compelling case if we had removed these transects.

6. Conclusions

[52] We were able in this study to confirm some concepts and question some others:

[53] 1. Mean shallow slab dip is 32° (between 0 and 125 km) and mean deep slab dip is 58° (deeper than 125 km), with positive variations near edges of the order of 10°.

[54] 2. There is an excellent correlation between slab dip and upper plate strain. Back-arc spreading is observed for deep dips larger than 51°, whereas back-arc shortening occurs only for deep dips less than 31°.

[55] 3. Slabs are steeper beneath oceanic upper plates (70 ± 20°) than beneath continental ones (50 ± 20°).

[56] 4. There is a good correlation between slab dip and absolute motion of overriding plate, as well as (in a least measure) absolute motion of the arc/trench. The correlation is even better when the slab lies on, or furthermore penetrates through, the 670 km discontinuity.

[57] 5. Slab dip correlates neither with the slab pull force, nor the age or the thermal parameter of the subducting plate.

[58] These observations suggest that forces originating from mantle flow, mantle viscosity contrast, bending forces or plate-motion-derived forces may prevail to counterbalance the slab pull force in the control of the slab dip. The manner in which the nature, strain or absolute motion of the upper plate interacts with the slab dip is still a matter of debate

and needs to be tested through experimental modeling. Nevertheless, we must admit that upper plate absolute motion correlates with slab dip, upper plate strain or nature, so that we can infer some primary control from this factor.

Acknowledgments

[59] This research was supported by the CNRS-INSU DyETI program "Dynamics of Subduction." We thank all our colleagues who participated in this program for the numerous discussions and debates. We really appreciated the constructive comments by the two reviewers Clint Conrad and Jeroen van Hunen as well as the associate editor Peter van Keken. Marc-André Gutscher kindly reviewed the grammar and word usage from the earlier version. All of them greatly helped us in improving the manuscript.

References

Barazangi, M., and B. L. Isacks (1976), Spatial distribution of earthquakes and subduction of the Nazca plate beneath South America, *Geology*, *4*, 686–692.

Bautista, C. B., M. L. P. Bautista, K. Oike, F. T. Wu, and R. S. Punongbayan (2001), A new insight on the geometry of subducting slabs in northern Luzon, Philippine, *Tectonophysics*, *339*, 279–310.

Bellahsen, N., C. Faccenna, and F. Funiciello (2005), Dynamics of subduction and plate motion in laboratory experiments: Insights into the "plate tectonics" behavior of the Earth, *J. Geophys. Res.*, *110*, B01401, doi:10.1029/2004JB002999.

Bijwaard, H. (1999), Seismic travel-time tomography for detailed global mantle structure, Ph.D. thesis, 181, 178 pp., Utrecht Univ., Utrecht, Netherlands.

Bostock, M. G., and J. C. VanDecar (1995), Upper mantle structure of the northern Cascadia subduction zone, *Can. J. Earth Sci.*, *32*, 1–12.

Cadek, O., and L. Fleitout (2003), Effect of lateral viscosity variations in the top 300 km on the geoid and dynamic topography, *Geophys. J. Int.*, *152*, 566–580.

Carlson, R. L. (1995), A plate cooling model relating rates of plate motion to the age of the lithosphere at trenches, *Geophys. Res. Lett.*, *22*(15), 1977–1980.

Carlson, R. L., T. W. C. Hilde, and S. Uyeda (1983), The driving mechanism of plate tectonics: Relation to age of the lithosphere at trench, *Geophys. Res. Lett.*, *10*, 297–300.

Conrad, C. P., and B. H. Hager (1999), Effects of plate bending and fault strength at subduction zones on plate dynamics, *J. Geophys. Res.*, *104*, 17,551–17,571.

Conrad, C. P., and C. Lithgow-Bertelloni (2002), How mantle slabs drive plate tectonics, *Science*, *298*, 207–209.

Conrad, C. P., S. Bilek, and C. Lihtgow-Bertelloni (2004), Great earthquakes and slab pull: Interaction between seismic coupling and plate-slab coupling, *Earth Planet. Sci. Lett.*, *218*, 109–122.

Cross, T. A., and R. H. Pilger (1982), Controls of subduction geometry, location of magmatic arcs, and tectonics of arc and back-arc regions, *Geol. Soc. Am. Bull.*, *93*, 545–562.

Doglioni, C., P. Hrabaglia, S. Merlini, F. Mongelli, A. Peccerillo, and C. Piromallo (1999), Orogens and slabs vs. their direction of subduction, *Earth Sci. Rev.*, *45*, 167–208.

Eberhart-Phillips, D., and M. Reyners (2001), A complex, young subduction zone imaged by three-dimensional seismic velocity, Fiordland, New Zealand, *Geophys. J. Int.*, *146*, 731–746.

Engdahl, R., R. van der Hilst, and R. Buland (1998), Global teleseismic earthquake relocation with improved travel times and procedures for depth determination, *Bull. Seismol. Soc. Am.*, *88*, 722–743.

Forsyth, D. W., and S. Uyeda (1975), On the relative importance of the driving forces of plate motion, *Geophys. J. R. Astron. Soc.*, *43*, 163–200.

Fujiwara, T., C. Tamura, A. Nishizawa, K. Fujioka, K. Kobayashi, and Y. Iwabuchi (2000), Morphology and tectonics of the Yap trench, *Mar. Geophys. Res.*, *21*, 69–86.

Fukao, Y., S. Widiyantoro, and M. Obayashi (2001), Stagnant slabs in the upper and lower mantle transition region, *Rev. Geophys.*, *39*, 291–323.

Furlong, K. P., D. S. Chapman, and P. W. Alfeld (1982), Thermal modeling of the geometry of subduction with implications for the tectonics of the overriding plate, *J. Geophys. Res.*, *87*, 1786–1802.

Gorbatov, A., S. Widiyantoro, Y. Fukao, and E. Gordeev (2000), Signature of remnant slabs in the North Pacific from P-wave tomography, *Geophys. J. Int.*, *142*, 27–36.

Gripp, A. E., and R. G. Gordon (2002), Young tracks of hotspots and current plate velocities, *Geophys. J. Int.*, *150*, 321–361.

Gutscher, M., and S. M. Peacock (2003), Thermal models of flat subduction and the rupture zone of great subduction earthquakes, *J. Geophys. Res.*, *108*(B1), 2009, doi:10.1029/2001JB000787.

Gutscher, M.-A., and S. Lallemand (1999), Birth of major strike-slip fault in SW Japan, *Terra Nova*, *11*, 203–209.

Hager, B. H., and R. J. O'Connell (1978), Subduction zone dip angles and flow driven by plate motion, *Tectonophysics*, *50*, 111–133.

Hall, R., and W. Spakman (2002), Subducted slabs beneath the eastern Indonesia-Tonga region: Insights from tomography, *Earth Planet. Sci. Lett.*, *201*, 321–336.

Heuret, A., and S. Lallemand (2005), Plate motions, slab dynamics and back-arc deformation, *Phys. Earth Planet. Inter.*, *149*, 31–51.

Jarrard, R. D. (1984), Prediction of continental structural style from plate tectonic parameters (abstract), *Eos Trans. AGU*, *65*, 1095.

Jarrard, R. D. (1986), Relations among subduction parameters, *Rev. Geophys.*, *24*(2), 217–284.

Jordan, T. E., B. L. Isacks, R. W. Allmendinger, J. A. Brewer, V. A. Ramos, and C. J. Ando (1983), Andean tectonics related to the geometry of subducted Nazca plate, *Geol. Soc. Am. Bull.*, *94*, 341–361.

Kirby, S. H., S. Stein, E. A. Okal, and D. C. Rubie (1996), Metastable mantle phase transformations and deep earthquakes in subducting oceanic lithosphere, *Rev. Geophys.*, *34*(2), 261–306.

Lagabrielle, Y., J. Goslin, H. Martin, J. L. Thirot, and J.-M. Auzende (1997), Multiple active spreading centers in the hot North Fiji Basin (SW Pacific): A possible model for Archean ocean dynamics?, *Earth Planet. Sci. Lett.*, *149*, 1–13.

Lallemand, S. (1998), Possible interaction between mantle dynamics and high rates of arc consumption by subduction processes in Circum-Pacific area, in *Mantle Dynamics and Plate Interactions in East Asia*, *Geodyn. Ser.*, vol. 27, pp. 1–9, edited by M. F. J. Flower et al., AGU, Washington, D. C.

Lallemand, S., Y. Font, H. Bijwaard, and H. Kao (2001), New insights on 3-D plates interaction near Taiwan from tomo-

graphy and tectonic implications, *Tectonophysics*, *335*, 229–253.

Luyendyk, B. P. (1970), Dips of downgoing lithospheric plates beneath island arcs, *Geol. Soc. Am. Bull.*, *81*, 3411–3416.

McNutt, M. K. (1984), Lithospheric flexure and thermal anomalies, *J. Geophys. Res.*, *89*, 11,180–11,194.

Molnar, P., and T. Atwater (1978), Interarc spreading and Cordilleran tectonics as alternates related to the age of subducted oceanic lithosphere, *Earth Planet. Sci. Lett.*, *41*, 827–857.

Müller, R., W. Roest, J.-Y. Royer, L. Gahagan, and J. Sclater (1997), Digital isochrons of the world's ocean floor, *J. Geophys. Res.*, *104*, 3211–3214.

Pankow, K. L., and T. Lay (1999), Constraints on the Kurile slab from shear wave residual sphere analysis, *J. Geophys. Res.*, *104*, 7255–7278.

Pardo, M., and G. Suàrez (1995), Shape of the subducted Rivera and Cocos plates in southern Mexico: Seismic and tectonic implications, *J. Geophys. Res.*, *100*, 12,357–12,373.

Parsons, T., A. M. Trehu, J. H. Luetgert, K. Miller, F. Kilbride, R. E. Wells, M. A. Fisher, E. Flueh, U. S. Brink, and N. I. Christensen (1998), A new view into the Cascadia subduction zone and volcanic arc: Implications for earthquake hazards along the Washington margin, *Geology*, *26*, 199–202.

Ranero, C. R., J. Phipps Morgan, K. McIntosh, and C. Reichert (2003), Bending-related faulting and mantle serpentinization at the Middle America trench, *Nature*, *425*, 367–373.

Replumaz, A., H. Karason, R. D. van der Hilst, J. Besse, and P. Tapponnier (2004), 4-D evolution of SE Asia's mantle from geological reconstructions and seismic tomography, *Earth Planet. Sci. Lett.*, *221*, 103–115.

Ricard, Y., C. Doglioni, and R. Sabadini (1991), Differential rotation between lithosphere and mantle: A consequence of lateral viscosity variations, *J. Geophys. Res.*, *96*, 8407–8415.

Ruff, L., and H. Kanamori (1980), Seismicity and the subduction process, *Phys. Earth Planet. Inter.*, *23*, 240–252.

Schellart, W. P. (2005), Influence of the subducting plate velocity on the geometry of the slab and migration of the subduction hinge, *Earth Planet. Sci. Lett.*, *231*(3–4), 197–219.

Smith, G. P., D. A. Wiens, K. M. Fischer, L. M. Dorman, S. C. Webb, and J. A. Hildenbrand (2001), A complex pattern of mantle flow in the Lau backarc, *Science*, *292*, 713–716.

Turcotte, D. L., and G. Schubert (1982), *Geodynamics: Applications of Continuum Physics to Geological Problems*, 450 pp., John Wiley, Hoboken, N. J.

Uyeda, S., and H. Kanamori (1979), Back-arc opening and the mode of subduction, *J. Geophys. Res.*, *84*, 1049–1061.

Vlaar, N. J., and M. J. R. Wortel (1976), Lithosphere aging, instability and subduction, *Tectonophysics*, *32*, 331–351.

Xu, J., and Y. Kono (2002), Geometry of slab, intraslab stress field and its tectonic implication in the Nankai trough, Japan, *Earth Planets Space*, *54*, 733–742.

Yang, T. F., T. Lee, C.-H. Chen, S.-N. Cheng, U. Knittel, R.-S. Punongbayan, and A.-R. Rasdas (1996), A double island arc between Taiwan and Luzon: Consequence of ridge subduction, *Tectonophysics*, *258*, 85–101.

Yogodzinski, G. M., J. M. Lees, T. G. Churikova, F. Dorendorf, G. Wöerner, and O. N. Volynets (2001), Geochemical evidence for the melting of subducting oceanic lithosphere at plate edges, *Nature*, *409*, 500–504.